scientific reports

Check for updates

OPEN

Comparative characterization of leather from different tanning processes as a contribution for a sustainable development of the leather industry

Sara Ferraris[1]✉, Francesca Gamna[1], Thomas Luxbacher[2], Giacomo Maculotti[3], Lorenzo Giorio[3], Jasurkhuja Kholkhujaev[3], Gianfranco Genta[3], Maurizio Galetto[3], Andrea Sarnataro[4], Marco Nogarole[4] & Claudia Florio[4]

Leather is a fully biobased material (100% biodegradable organic material, with collagen as the main constituent), derived from food industry byproducts (animal skin from butchery), which represents an excellence for the Italian industry (in the last years the production value reached 4.6 billion euros and an export of 3.2 billion euros) and a highly sustainable material. However, its production is still strongly handicraft, traditional and unfortunately based on the employment of toxic chemicals, such as chromium and glutaraldehyde. A deep knowledge of the tanning process and of the specific features of leather coming from different processing routes is crucial for the design and development of innovation in the field for a more sustainable and knowledge-based production. In this contest, the impact of tanning process on the surface reactivity of leather plays a crucial role. In the present research well established characterizations (optical microscopy, shrinkage temperature, wettability, metal content, infrared spectroscopy and X-ray diffraction) and new and unconventional methods for the leather field (surface topography, instrumented indentation and zeta potential electrokinetic measurements) were applied and optimized for the characterization of leather samples from traditional (e.g. Chrome and Glutaraldehyde) and innovative (e.g. vegetable, carbamoyl sulphate, starch, aluminum, zeolite, triazine and Olive Mill Wastewaters -OMW) tanning processes. The suitability of the characterization protocol for the in-depth investigation and comparison of leather samples from different processing has been demonstrated highlighting its applicability for a knowledge-based innovation in the leather field.

Keywords Leather, Surface characterization, Zeta potential, Instrumented indentation, tanning

Leather represents one of the Italian excellences and is a product of small to medium size tanning industries characterized by the combination of high technological process and strong handicraft creativity[1].

Italian tanning industry counts 1146 companies with 18,030 employees for 110 million square meters of finished leather with a production value of 4.6 billion euros and an export of 3.2 billion euros in 2022[2].

Leather is a fully bio-based material (100% biodegradable organic material, with collagen as the main constituent) derived from food industry byproducts and recovered by tanneries[1]. In this sense it represents a more sustainable and green material compared to synthetic polymers derived from fossil sources. However, tanning industry is still based on the use of toxic reagents, such as chromium salts or glutaraldehyde, at the basis of conventional tanning processes, and innovation actions should be made in order to substitute these auxiliary agents with more environmentally friendly ones.

The sustainable management of leather waste and the valorisation of collagen obtained from these by-products have gained increasing interest. Several studies have demonstrated that collagen can be efficiently extracted from

[1]Department of Applied Science and Technology, Politecnico di Torino, Turin, Italy. [2]Anton Paar GmbH, Graz, Austria. [3]Department of Management and Production Engineering, Politecnico di Torino, Turin, Italy. [4]Stazione Sperimentale per l'Industria delle Pelli e delle Materie Concianti (SSIP)-Italian Leather Research Institute, Naples, Italy. ✉email: sara.ferraris@polito.it

deteriorated leather artifacts[3], raw hide trimmings[4] and solid waste from the leather industry[5] making it a valuable raw material for biomedical, pharmaceutical, and cosmetic applications. The extraction of collagen from waste leather production not only contributes to circular economy models but also helps in reducing environmental impact by minimizing solid waste disposal. For instance, optimized methods for collagen extraction from raw hide trimmings have resulted in high-value products such as gelatin and collagen hydrolysate, which are widely used in various industries[4,6,7]. Furthermore, research has demonstrated that collagen extracted from leather production waste can form hydrogels suitable for biomedical applications, highlighting its potential in tissue engineering and regenerative medicine[5].

The change of tanning agents can have an impact on the whole tanning process, which needs to be deeply investigated in order to guarantee the expected performances of the final leather. Moreover, the continuous search for alternative tanning systems, to ensure growing levels of sustainability and biodegradability, may cause novel technical challenges and novel categories of leather defects, which have to be known and avoided in the innovation and optimization of the tanning process[8].

Recent research has increasingly focused on the development of more sustainable tanning methods, driven by the need to reduce the environmental impact of conventional processes, particularly those involving hazardous chemicals[9]. The introduction of alternative tanning agents, such as plant-derived compounds and enzymatic treatments, mineral-based tanning agents aims to improve biodegradability and lower pollution levels[10–14]. Furthermore, advancements in cleaner production strategies emphasize the reduction of waste and resource consumption, aligning with global efforts towards more environmentally responsible leather manufacturing[8].

Therefore, in order to guarantee the high-quality performance of leather, compared with alternative emerging materials, a strict monitoring of the most crucial parameters of the production phases and the deriving surface and bulk properties of the material is of mandatory importance. Ensuring a balance between innovation and performance remains essential to overcoming the technical challenges associated with novel tanning approaches [11].

Scanning Electron Microscopy equipped with Energy Dispersive Spectroscopy (SEM-EDS), Infrared Spectroscopy (IR), Gas Chromatography (GC), X-ray fluorescence (XRF), differential scanning calorimetry and thermogravimetry (DSC/TG) were used as analytical techniques mainly for the investigation of leather defects[15–17].

The zeta potential is a powerful parameter for the investigation of functional groups, acid/basic behavior, colloidal stability of materials for catalysis[18], electrophoretic deposition, water purification, food, textiles, cosmetic, lubricant, nanotechnology, medicine[19] and biomaterials applications[20,21].

Electrophoretic measurements of zeta potential are the most diffused and applied for the evaluation of colloidal stability of suspensions, nanoparticles and catalysts[22]. However, streaming potential measurements are now getting increasing interest for the evaluation of isoelectric point and zeta potential of bulk materials in many application fields[23].

Some papers concerning the isoelectric points of leathers after different processing[24–27] can be found in the scientific literature, but few of them report an in-depth discussion on the whole pH titration curve, confirming the necessity of proper measurement design and optimization in the leather field[28].

In fact, isoelectric point and surface charge in function of pH (titration curve) of leathers can give indications of the functional groups exposed by the material surface at different stage of processing, as well as after tanning with different products. These studies can give an in-depth investigation of the tanning process and the basis for tanning innovation.

Surface topography quality is of utmost relevance to assess the quality leather. Many sectors, e.g. premium or automotive, require strict tolerances of surface defects (in size and extension), and overall homogeneity of the manufactured leather products. These, can be due to ante- and post-mortem marks which can affect the overall aesthetic appearance[29,30] while altering tactile and mechanical properties[31] of the product. Accordingly, qualitative[29] and quantitative[31] inspections are commonly reported to evaluate the quality of tanned products. The former is typically carried out by cameras[29], while the other require surface topography measuring instruments[31,32], that enable the evaluation of surface topography parameters[33]. Such evaluations are essential to provide design tolerances and objective evaluation methods of raw and processed materials. Tanning process of hides and skins to produce leather can relieve such defects, thus improving overall aesthetic, tactile and mechanical quality of the product. The latter is strongly affected by geometrical, i.e. topographical, singularities which can act as notches liable of reducing the mechanical strength, conventionally evaluated by tensile tests on ad-hoc shaped specimens[34–36]. However, other alternatives to estimate the mechanical response, which are faster and require less sample preparation are available in the literature, i.e. instrumented indentation test (IIT), but are unreported for leather. IIT is a non-conventional depth-sensing hardness test allowing the evaluation of estimate of the Young modulus, hardness, creep and relaxation of materials[37–39].

In the present research some conventional techniques, such as evaluation of the shrinkage temperature and metal content, contact angle measurements, Fourier Transformed Infrared spectroscopy, X-Ray Diffraction, surface topography characterization and some new approaches, such as instrumented indentation test and zeta potential streaming potential measurements have been applied to leather samples to obtain an thorough characterization and comparison of materials from traditional (e.g. Chrome and Glutaraldehyde) and innovative (e.g. vegetable, starch and Olive Mill Wastewaters -OMW) tanning processes, which is currently missing in the literature. The explored techniques aim to highlight differences among the different tanned leathers, correlate these differences with the tanning mechanism, predict and optimize the results of innovative processing.

In fact, tanning process is based on collagen crosslinking exploiting the reaction between tanning agent and collagen functional groups. The investigation of functional groups exposed in the tanned leather gives information about the groups exploited in tanning. Moreover, investigations related to collagen structure and leather stability are related to the effectiveness of the tanning mechanism.

An in-depth characterization of alternative tanning technologies, with reduced employment of toxic agents such as chromium or glutaraldehyde or based on molecules derived from byproducts, allows a critical comparison among the technique and also the optimization of innovative procedures to obtain leather products with the same quality of traditional ones but with lower environmental impact.

Among the alternatives in the literature[40], demonstrated the use of innovative and environmentally friendly tanning agents such as β-cyclodextrin-based tanning agents, which show excellent results in terms of retraction temperature and xeno-test resistance. The work of Hao et al.[41] studied other organic-based tanning agents such as 1,3,5-tris(hydroxyethyl)-s-triazine, which, in addition to a very competitive shrinkage temperature, also exhibits interesting antimicrobial properties. Wang et al.[42] obtained innovative tanning agents with a soluble starch base, and also achieved excellent shrinkage temperature and high resistance to yellowing. Hao et al.[43] showed how the use of ethylene glycidyl ether grafted with dialdehydic maize starch in tanning resulted in an innovative tanning agent with excellent physical properties, superior to those of other commercial chrome-free tanning agents such as F-90. Several works[42,44–46] considered the functionalization of collagen extracts from waste from the tanning industry to obtain a tanning agent and optimize the circular process.

The presence of these numerous studies in the literature demonstrates the importance of active research to find chrome-free alternatives for more environmentally friendly tanning.

Materials and methods

Leather samples

The following intermediate leather samples in the wet state were considered:

1. Cr_wet: tanned bovine leather—chrome based tanning.
2. GLU_wet: tanned bovine leather—glutaraldehyde based tanning.
3. VEG_wet: tanned bovine leather—vegetable tanning.
4. Carb Sulph_wet: tanned bovine leather—carbamoyl sulphonate based tanning.
5. Starch_wet: tanned bovine leather—dialdehyde starch-based tanning.
6. Al_wet: tanned bovine leather—aluminum salts-based tanning.
7. Zeo_wet: tanned bovine leather—modified zeolite A-based tanning.
8. OMW_wet: tanned bovine leather—polyphenols from Olive Mill Wastewaters—based tanning.
9. Tria_wet: tanned bovine leather—triazine-based tanning.

The first three samples have been considered as reference materials obtained using traditional tanning agents, for the optimization of the measurement setup and for the comparison with innovative and sustainable materials. Samples 4–9 can be considered as example of innovative tanning processes to evaluate the ability of the proposed techniques to properly highlight differences among these typologies of materials.

Since triazine based tanning process are actually often limited to the processing of ovine leather and require specific finishing routes, traditional characterizations (shrinkage temperature, metal content, wettability and optical microscopy) have not been applied to this sample in the present research. This tanning can be considered as non-traditional but quite old and tested to be included among the most innovative. On the other hand, more innovative characterizations have instead been considered in order to better highlight the ability of proposed methodologies to investigate leather from different tanning processes and all the available tannings have been explored to make the test more solid.

Shrinkage temperature

In leather technology, shrinkage temperature (Ts) it is a parameter indicative of hydrothermal stability of leather and is widely used to compare the capability of different tanning agents to stabilize derma structure.

Ts values of the above described samples, have been evaluated according to the official test method to assess the shrinkage temperature of leather, described into the standard ISO 3380:2015 (IULTCS/IUP 16)[47]: that a rectangular sample is immersed in a vessel fixed in iso-strain conditions in a specimen holder at a temperature ramp of 2 °C ± 0,2 °C from room temperature till boiling. One clamp of the holder is moveable and connected with a dial comparator that measures the reciprocal movement of clamps with an accuracy of 0,15 mm. When shrinkage occurs, the index moves, and the temperature that correspond to a contraction equal to 0,3% is noted, indicating the hydrothermal stability of the samples.

Metal content

The metal content was determined in accordance with ISO 17072-2:2022[48], after acid digestion of the leather samples and analysis of the extracted solution using an inductively coupled plasma mass spectrometer (ICP-MS), Thermo Fisher ICAPRQ. For the preparation, in accordance with ISO 4044, the leather samples to be tested, if wet, are first dried in an oven at 50 °C, then approximately 1 g is weighed and 10 ml to 20 ml of a mix of acids are added composed of H_2SO_4, HNO_3 and $HClO_4$; it is left to react in the digester until digestion is complete; then it is cooled and re-dissolved with H_2O in a flask to 100 ml. In order to monitor any contaminants, before each sample sequence, the ternary acid solution used, which is identified as blank, is analyzed in the same way as the samples. Once the instrumental parameters have been set, the samples are compared with solutions of metals of known concentration.

Wettability

The wettability of the sample surface was estimated by measuring the contact angle, according to the ASTM standard Test Method for Surface Wettability D 724–99[49], using a *FIBRO System AB - Mod. PGX* Pocket Goniometer. Contact angle has been evaluated dynamically, within 0 and 10 s from the impact of water drops,

having a volume of about 2 µl, on leather surface; the evaluation of the contact angle in dynamic mode, together with the measurement of the variation over time of other parameters of the micro-droplet (such as its volume, base and height), allows to effectively evaluate the dynamics of water absorption and other liquids from the leather surface[50–52].

Fourier transformed infrared spectroscopy in attenuated total reflectance (FTIR-ATR)

The main chemical groups and eventual effects of processing and drying were evaluated by means of Fourier Transformed Infrared Spectroscopy in Attenuated Total Reflectance mode (FTIR-ATR, Nicolet iS50 FTIR Spectrometer, Thermo Scientific, USA).

X-ray diffraction

X-Ray Diffraction (XRD) was used in order to characterize the effect of tanning on collagen structure. Measurements were performed in Bragg-Brentano configuration (XRD – PANalytical X'Pert Pro PW 3040160 Philips, Malvern Panalytical, Egham, United Kingdom) and the patterns were analyzed by XPERT High Score software.

Topographical characterization

Surface topography has been qualitatively investigated by optical microscopy, and quantitatively at different scale by SEM, at nano scale, and by topographical microscope, at micro scale.

The surface and cross section of the samples were analyzed through an SPZ 10 Optika stereomicroscope, which allows working with reflected and transmitted light; the cross sections were obtained with the use of a blade and, where necessary, with the aid of a microtome, which allows obtaining transversal sections with a thickness of 30 µm, which are placed on a glass slide for subsequent observation.

Topographical quantitative characterization was carried out in the DIGEP Min4Lab facilities in a metrological room (controlled temperature 20 °C ± 1 °C) by means of a state-of-the-art Coherence Scanning Interferometer NewView™ 9000 by Zygo[53,54]. The instrument was equipped with a 5.5× objective with Numerical Aperture of 0.15, a Field-of-View (FoV) of (1.56 × 1.56) mm and a squared pixel of 1.56 µm side, and a measurement uncertainty of 10 nm[55,56]. Each of the 9 samples was measured in at least 5 different randomly selected locations, each of whom was independently characterized to provide replications. The quantitative characterization has been carried out as per relevant standard, namely ISO 25178-2[33] and ISO 25178-3[57] by means of the software MountainsLab v8. Specifically, the Scale Limited surface (SL-Surface) was characterized, applying S-filter, for noise removal and bandwidth matching[58], and the L-filter, for waviness elimination, as robust Gaussian filters[59] with nesting index of 5 µm and 500 µm, respectively[57]. Both filters have been applied after the correction of planarity by means of the application of a least-square plane form correction by a F-operator. Both field and features parameters have been evaluated. The considered areal field parameters are height parameters, describing the average (Sa), standard deviation (Sq) and the third and fourth statistical moment of the height distribution, i.e. the Skewness Ssk and the Kurtosis Sku. Additionally, the maximum peak height, Sp, and the maximum pit depth, Sv, both evaluated with respect to the mean plane, have been reported, along with their sum, i.e. the maximum height $Sz = Sp + Sv$. Furthermore, the areal field parameters describing topographic autocorrelation, i.e. the autocorrelation length Sal and the texture aspect ratio Str have been reported. These, respectively, represent how fast the topographic height autocorrelation function decays, conventionally values smaller than 0.2% indicates a-periodic surface, and if such spatial correlation has any preferential orientation, thus informing on the topographic isotropy, conventionally for Str > 50%[60]. The field hybrid parameters describing the root mean square gradient (Sdq) of the topography, and developed interfacial area ratio (Srd) have been assessed to describe, respectively, how quickly the topography changes and the relative extent of the texture with respect to the evaluation area. Last, features have been characterized. In particular, dales, which can be linked to skin pores have been identified by watershed segmentation, and quantitatively estimated in terms of the average areal extension $\bar{A}_p$, the standard deviation of such area, $s(A_p)$, both evaluated on each FoV, the maximum pore depth $z_{max,p}$ and the mean pore depth $\bar{z}_{max,p}$ over the evaluation area[61,62].

Treatment effect on the topographical appearance and characterization has been investigated by means of non-parametric statistics, due to the highly non-normal distribution of the considered parameters[63]. Accordingly, the Mood's median test[64] has been carried out to quantitatively assess if the considered tanning processes systematically affect the topography.

Instrumented indentation test

Instrumented Indentation Test (IIT) has been carried out by means of a state-of-the-art indentation platform Anton Paar STeP6 equipped with a micro-IIT head MCT^3 in the metrological room of the Mind4Lab[65,66]. IIT consists of applying a loading-holding-unloading force-controlled cycle with a Berkovich indenter on the sample, and the measurement throughout the cycle the applied force (F) and the indenter displacement (h) in the sample. By the analysis of the indentation curve (IC), i.e. the $F(h)$ curve, provided the calibration[67–69] of the frame compliance, to remove elastic displacement of the indentation machine, and of the indenter geometry, to associate to the penetration the projected contact area of the indenter, it is possible to obtain estimates of the Young modulus, by means of the Indentation modulus E_{IT}, and evaluate the indentation hardness H_{IT}[37–39]. Micro-IIT has been performed applying a maximum force of 500 mN with a loading and unloading of 5 s each, and a holding of 60 s aimed at compensating and stabilizing room temperature creep of the material[70]. Matrixes of 4 × 4 indentations with a x-y spacing of 500 µm have been performed on the 9 tanned samples and ANOVA[71] has been resorted to investigate the systematic effect of different tanning treatment on the mechanical characterization results. The application of IIT to replace conventional and standard tensile test on leather to

asses quality is unreported to the best of the authors' knowledge and provides a methodological alternative highly interesting for ease of set-up and execution for quality control.

Zeta potential titration curves

The zeta potential as a function of pH of a dilute aqueous solution and the isoelectric point (IEP) were determined by the streaming potential measurement of leather samples at the wet state (SurPASS, Anton Paar). The zeta potential ζ is calculated from the measured streaming potential U_{str} using the classical Smoluchowski Equation[72],

$$\zeta = \frac{dU_{str}}{d\Delta p} \frac{\eta}{\varepsilon_r \varepsilon_0} \kappa_B \quad (1)$$

with Δp—pressure difference between both ends of a capillary flow channel, η—dynamic viscosity, ε_r – relative permittivity of the test solutions, ε_0—vacuum permittivity, and κ_B—electric conductivity of the bulk solution.

In order to measure the material at the wet state a cylindrical cell was used and the samples were chopped in small fragments (few mm each). A plug of chopped leather was formed in the cylindrical compartment of the measuring cell and supported at both ends by perforated disks. The aqueous test solution was then permeated across this sample plug. Measurements were performed with aqueous solutions of KCl at different ionic strength of 0.001 mol/l and 0.01 mol/las electrolytes to illustrate and better understand the possible effect of leather swelling on the zeta potential results. Since the electrolyte solution flows through the plug of chopped leather sample during the measurement, the resulting information can be correlated with the bulk properties of the material (all surfaces, i.e., skin and flesh sides, are in contact with the electrolyte)[73]. In order to explore the behavior of the material in a wide pH range (pH 3–9) the dosing unit of the instrument was used for an automatic titration. The titration was started at the native pH of the aqueous KCl solution and proceeded to low and high pH using 0.05 mol/l HCl and 0.05 mol/l NaOH, respectively, with a new plug of chopped leather for each pH range.

Results

Leather samples: macroscopic appearance

The product and morphological analysis, aided by the examination of the surface and sections of the five samples, using optical microscopy, highlighted the findings reported in Fig. 1.

The appearance of the grain was found to be clearly visible for the first three samples (made with traditional tannings), and for the last sample 8 (made with novel tanning agents Olive Mill Wastewaters based), suggesting the promising use of this type of new tanning system, in terms of product properties provided to the leather; for the same samples, the structure of the dermis was also found to be compact, with a dense fibrous network; on the contrary, the samples 4, 5 and 7 were found to be characterized by a partially abraded grain (depending on the typical processing and intended use of the samples); furthermore, for the samples 4, 5 and 7, a more linear and straight, rather intertwined, structure of the dermis fibers was highlighted; moreover for sample 4, some black spots highlighted the possible occurrence of leather defects, related to errors in the first phases of the tanning process. Intermediate surface and cross-section features were found for sample 6 (zeolite tanning based).

Shrinkage temperature (Ts)

As highlighted in Table 1, consistently with what was expected, the most stable sample, from a hydro-thermal profile, and therefore with higher shrinkage temperature values was found to be the first one (1_Cr_wet, chrome tanned); the other samples showed Ts values comparable to each other and with the value obtained for the sample tanned with glutaraldehyde, highlighting a reasonable capability of alternative tannings (such as the starch-based and Olive Mill Wastewaters based ones) to stabilize the collagen structure with good efficiency. A lower Ts value was found for the vegetable, aluminium and zeolite tanned sample.

In agreement with literature, various alternative tanning methods have demonstrated sufficient hydrothermal stability, although generally lower than chrome tanning. Studies on starch-based tanning have reported shrinkage temperatures exceeding 84 °C, particularly when using chemically modified starches, confirming their ability to effectively stabilize collagen[46].

A lower Ts value was found for the vegetable, aluminum, and zeolite tanned samples, which is consistent with previous studies reporting slightly reduced shrinkage temperatures for vegetable tannins and mineral-based systems. These findings align with recent trends in tanning research, where alternative processes, while not always reaching the thermal stability of chrome tanning, still provide adequate collagen stabilization and structural integrity for practical applications[44].

This comparison with literature supports the idea that a range of alternative tanning methods can be effectively employed, each with different impacts on the final material properties. While slight variations in shrinkage temperature are expected depending on the tanning agent used, the results confirm that several non-chrome approaches can offer viable solutions for leather processing, balancing performance and sustainability considerations.

Metal content

Based on the tanning metal content found (Table 1), it was possible to classify the analyzed samples, as follows, according to the standard UNI EN ISO 15987:2015[74], containing Key Definitions for the leather trade:

- the definition of Metal Free leather provides that the total concentration of Tanning Metals (Aluminium, Chromium, Iron, Titanium and Zirconium) must be found to be less than or equal to 0,1% (i.e. 1,000 mg/kg) expressed on the dry substance;

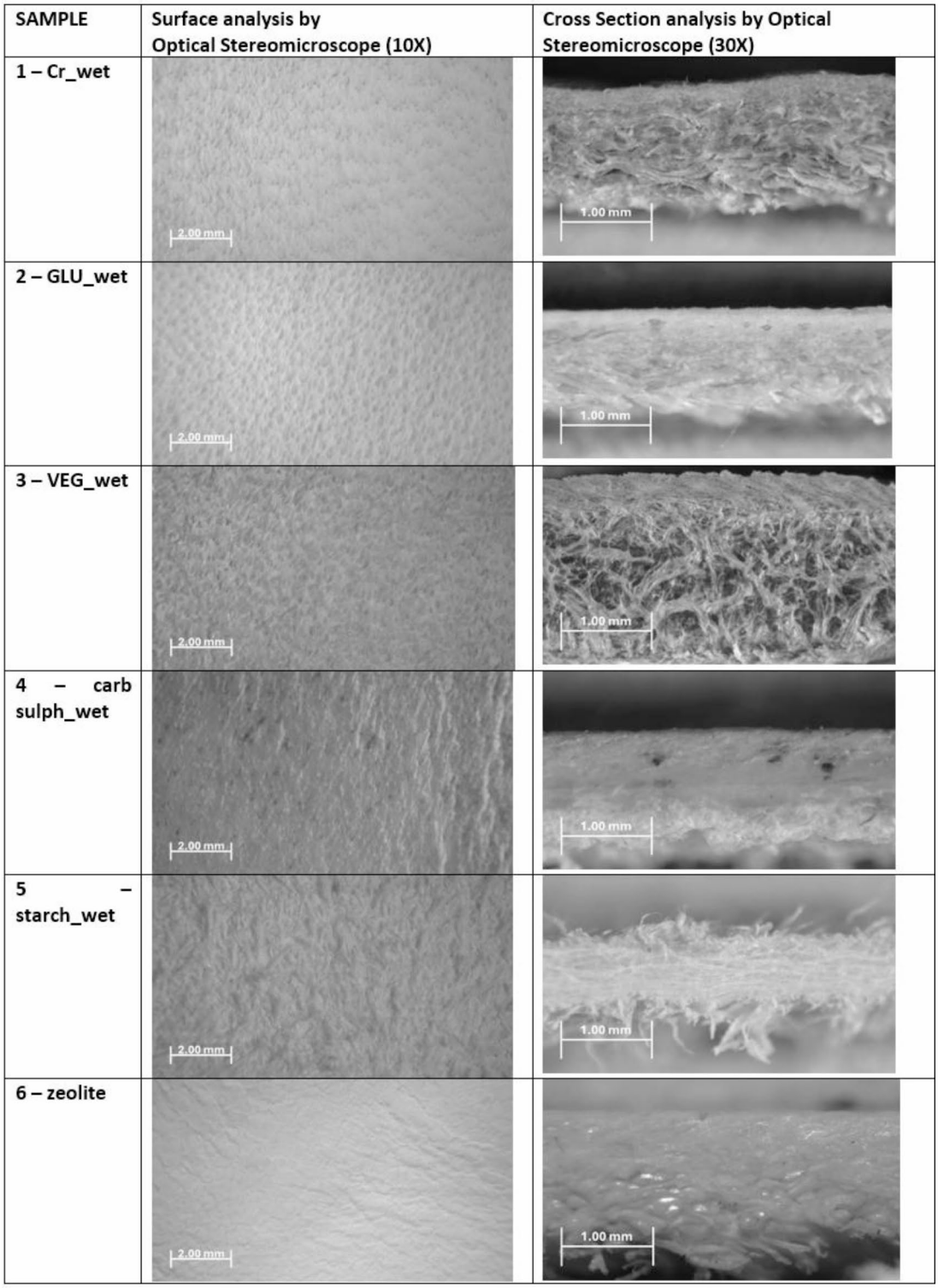


Fig. 1. Morphological analysis of samples surface and cross section.

- the definition of Chrome Free leather provides that the total concentration of Chromium must be found to be less than or equal to 0,1% (i.e. 1,000 mg/kg) expressed on the dry substance.

The results obtained highlighted that sample 1—Cr_wet cannot be defined nor as "chrome free" leather nor as "metal free" leather. On the other hand, sample 2—GLU_wet, sample 3—VEG_wet, sample 4—carb sulph_wet and sample 5—starch_wet can be defined as both "chrome free" and "metal free" leathers. Finally, sample 6—Al wet, sample 7—Zeo_wet and sample 8—OMW_wet, can be defined as "chrome free".

Test	Method/ standard	UOM	Values for sample							
			1—wet blue leather—chrome tanning	2—tanned leather—glutaraldehyde based tanning	3—vegetable tanned leather	4—tanned leather—organic based tanning agents	5—starch-based tanning agents	6—Zeolite	7—Alluminium	8—OMW
Average thickness	UNI EN ISO 2589:2016	mm	1.65	1.54	3.58	1.59	0.69	0.69	0.69	0.69
Shrinkage temperature	UNI EN ISO 3380:2015	°C	> 95	76	72	79	78	71	71	78
Hexavalent chromium	UNI EN ISO 17075-2:2017	mg/kg	< 3,0							
Total aluminium content	UNI EN ISO 17072-2:2019	mg/kg s.s.	2.28	3.95	21.5	9.77	91.3	18807.64	7427.83	1129.68
Total chromium	UNI EN ISO 17072-2:2019	mg/kg s.s.	2.965	2.82	3.17	2.03	< 0,02	111.73	53.72	11.98
Total iron content	UNI EN ISO 17072-2:2019	mg/kg s.s.	3.59	0.38	5.7	2.21	33.3	145.13	108.2	312.31
Total titanium content	UNI EN ISO 17072-2:2022	mg/kg s.s.	< 0,1	< 0,2	< 0,1	< 0,1	14.6	36.48	12.37	5.98
Total zirconium content	UNI EN ISO 17072-2:2022	mg/kg s.s.	0.98	0.56	0.95	0.55	0	0	0	0
Total tanning metals	UNI EN ISO 17072-2:2022	% s.s.	0.3	0.001	0.003	0.001	0.01	1.9	0.76	0.146
Classification	UNI EN ISO 15987:2023		Chrome leather	Metal free leather	Metal free leather	Metal free leather	Metal free leather	Chrome free leather	Chrome free leather	Chrome free leather

Table 1. Main technical, product and ecotoxicological features of the leather analyzed.

With a view to qualifying the characteristics of the samples, also on an eco-toxicological level, the hexavalent chromium content was also determined for the chrome tanned sample, in accordance with the standard UNI EN ISO 17075-2[75], the value of which was found to be lower than the prescribed limits for all the main intended uses of the material.

Wettability

Figure 2 shows the results obtained highlighted significant variability in the different cases examined; a particularly hydrophobic behavior was highlighted for sample 5, while for the others a certain hydrophilicity and permeability was found.

Fourier transformed infrared spectroscopy in attenuated total reflectance (FTIR-ATR)

Figure 3 reports FTIR-ATR spectra of the leather samples in the wet state both sides (Grain—g and Flesh—f) were tested and reported in the graphs.

The FTIR spectra provide insights into the molecular interactions and changes in collagen structure across different tanning processes. The characteristic amide bands (Amide A, B, I, II, and III) are present in all spectra, reflecting the preservation of the collagen backbone across the various tanning methods. These peaks are associated with specific molecular vibrations related to the peptide bonds of collagen, essential for understanding how the tanning agents affect the material.

Indeed, all leathers exhibit typical collagen absorption bands. The two amide bands (I-II) are due to C = O stretching, C-N stretch and NH deformation[76] and are found in all type of tanned leathers at 1638, 1540 cm^{-1}, respectively. Considering the Amide III band, collagen is characterised by three main peaks centred at 1284, 1240 and 1202 cm^{-1}[77]. These represent the structure of collagen (random coil or crystalline) and actually change according to the type of tanning[78]. Amide A peak (around 3300 cm^{-1}) is presented clearly in all the leathers due to hydrogen bonding. There are two addition bands presented in all leathers at 2920 cm^{-1} and 2850 cm^{-1}, which are related to lipids[79,80].

These bands were stronger on the upper (grained) surface than on the lower (flesh) surface of Cr and GA-tanned leather, suggesting a treatment with oils and other fats applied on the top surface[78]. A different amount of lipid on the top of the surface can be seen depending on the tanning of the leather. Indeed, the leathers tanned with VEG, Carb-sulf, and GLU, as well as Tria and Al, exhibit a less pronounced peak in this frequency band. This observation aligns with the contact angle study, which indicates a more hydrophilic surface for these three types of leather. In contrast, the organic-based tanning methods, such as starch and OMW, show a higher peak corresponding to the lipidic band. This results in more amorphous collagen structures, enhancing the flexibility and softness, particularly on the grain side.

X-ray diffraction

Figure 4 reports XRD spectra of the analyzed leather samples.

The main contributions in the XRD spectra of leathers can be found at 8° and 20°. The peak at about 8° relates to the characteristic intermolecular lateral packing within collagen fibrils and the peak at about 20° comes from the amorphous scattering, resulting from the unordered components of the collagen fiber[81,82].

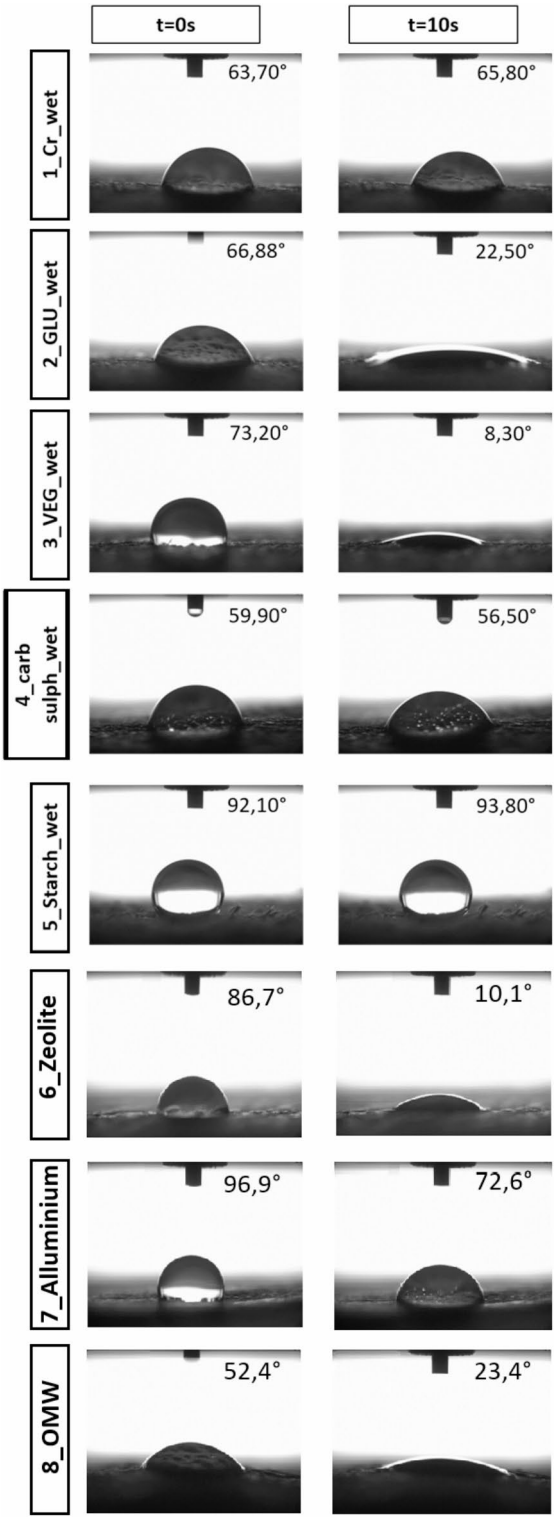


Fig. 2. Contact angle measurements at 0 and 10s.

The X-ray diffraction (XRD) analysis reveals clear structural differences between the various tanning agents used in the study. The chromium-tanned sample (Cr_wet) and glutaraldehyde-tanned samples (GLU_wet) exhibit distinct peaks, particularly at low angles, indicating a relatively crystalline structure. In contrast, the VEG_wet tanned samples show broader, less defined peaks, characteristic of amorphous structures, this suggests that these organic tanning methods lead to a more disordered molecular arrangement, which may influence the flexibility and permeability of the final material, probably because of water adsorption from the collagen chain[83]. The sulfur-based (Carb Sulph_wet) and starch-based (Starch_wet) samples also show relatively amorphous

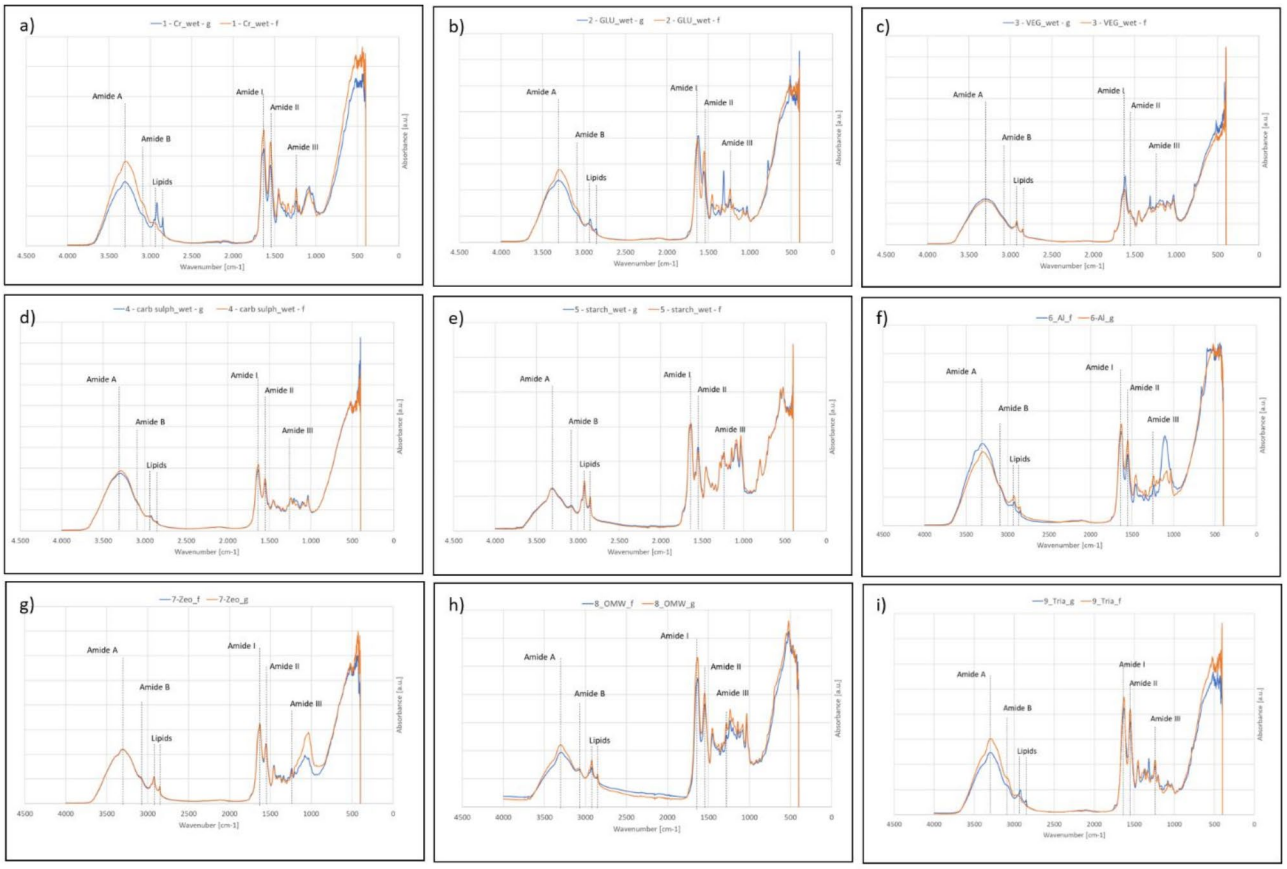


Fig. 3. FTIR ATR spectra of (**a**) 1—Cr_wet, (**b**) 2—GLU_wet, (**c**) 3—VEG_wet, (**d**) 4—carb sulph_wet and (**e**) 5—starch_wet, (**f**) 6—Al_wet, (**g**) 7—Zeo_wet, (**h**) 8_OMW_wet, (**i**) 9_Tria_wet.

characteristics, with moderate peaks indicating a lower degree of crystallinity compared to the chromium-tanned sample.

The aluminum-tanned sample (Al_wet) displays a much more ordered structure, with prominent peaks in the XRD pattern that reflect its crystalline nature. Similarly, the zeolite-based tanning method (Zeo_wet) produces sharp peaks at 8 degree. On the other hand, the OMW_wet sample and Tria_wet samples result in more amorphous structures, as indicated by their broad, low-intensity peaks. The lack of sharp peaks in these samples suggests a less ordered arrangement, which could lead to different functional characteristics such as increased flexibility or porosity, as indicated by topography and mechanical tests.

Topographical characterization

Topographical measurements have been carried out by means of CSI instrument as per Section "Topographical characterization" and Fig. 5 shows the qualitative appearance of the considered tanned hides. As it can be appreciated, conventional processes, i.e. 1—Cr_wet, 2—GLU_wet and 3—VEG_wet, show a uniform surface, with a limited height range and very few isolated features. Conversely, 5—starch_wet samples show a significantly irregular surface with fibers and pores; the 4—Carb Sulph_wet sample has an intermediate appearance. Specimens 6—Al_wet, 7—Zeo_wet, 8—OMW_wet and 9—Tria_wet present a uniform distribution of pores on the surface, with a decreasing height range moving from specimen 9 to specimen 6 (lowest height range).

Quantitative characterization has then been carried out as described in Sect. 2.7 and field and features parameters have been evaluated; box plots of the parameters are shown in Fig. 6. From the boxplots, preferred to interval plot to better highlight the non-normality of the parameters, consistent differences both in median and dispersion among the different treatments can be appreciated. Such differences are confirmed by the Mood's median test, which highlighted a systematic effect of the different tanning agents on all the considered topographical parameters at a confidence level of 95%. Specifically, starch tanned specimen shows a higher topographical roughness both as dispersion (Sq) and average (Sa). Starch and Vegetable presents highest peaks and deepest pores (Sp, Sv), which is well captured also by the feature parameters, i.e. in terms of average and standard deviation of the pore areas and the pores maximum depths, for which those two alternative sustainable tanning presents worst values. Furthermore, the great degree of variability, easily attributable to the fibers, can be well captured by the Sdq, which is again systematically higher for starch tanning. In general, topographies are random ($Sal < 0.2$) for all tanning processes, and isotropic ($Str > 50\%$) for specimen OMW, Cr_wet, GLU_wet, Starch_wet, Triazine, VEG_wet and Zeolite; the others specimens, however, present values for Str close to

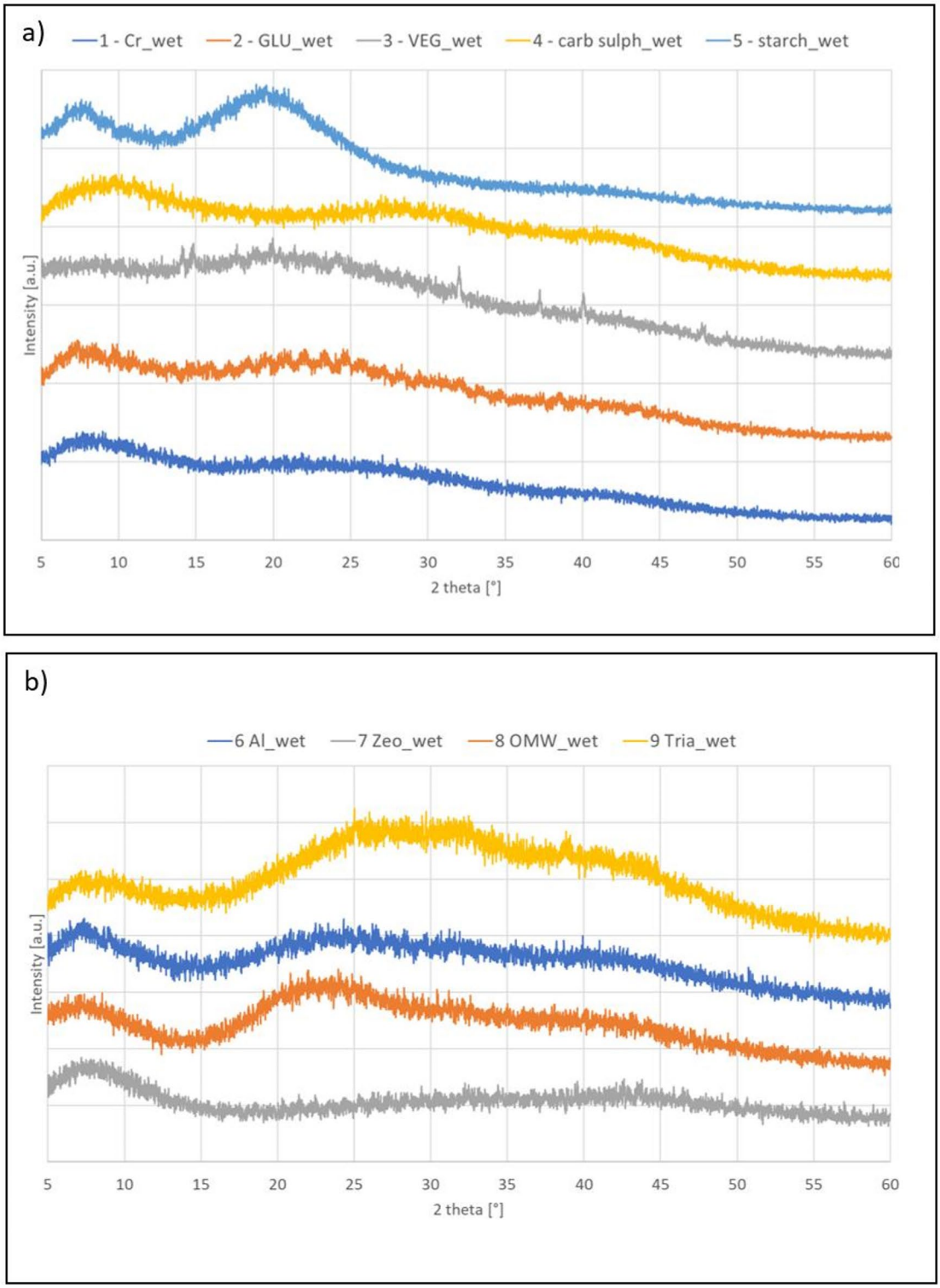


Fig. 4. XRD spectra of leather samples: (**a**) 1—Cr_wet, 2—GLU_wet, 3—veg_wet, 4—carb-sulph_wet, 5—starch_wet; (**b**) 6—Al_wet, 7—Zeo_wet, 8—OMW_wet, 9—Tria_wet and.

50%. In general, the innovative and sustainable tanning agents result in a rougher and less reproducible surface topography.

Instrumented indentation test

Figure 7 shows a representative result of the IC performed on the samples. Due to the highly unstable, wet and ease to decay, i.e. prone to grow molds, of the vegetable-tanned samples, indentation could not be

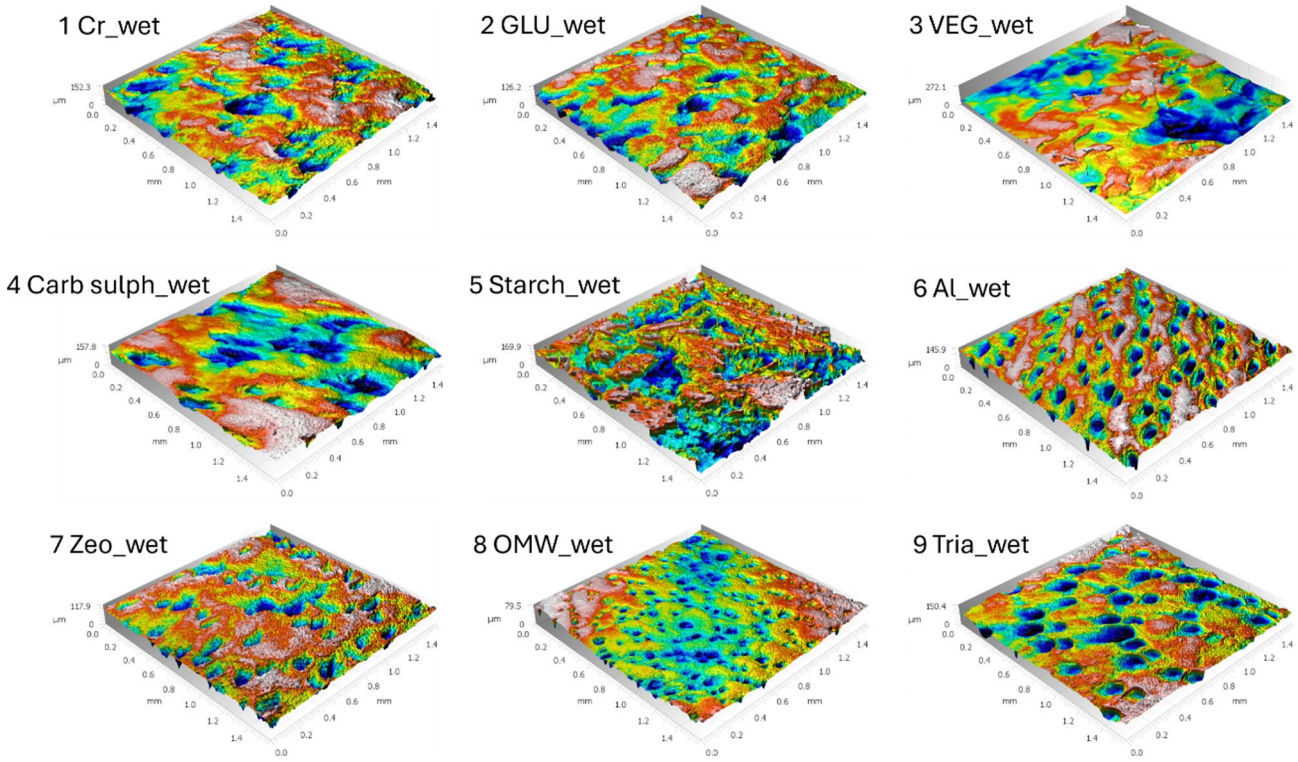


Fig. 5. Measured topographies in true colours.

carried out on it. Qualitatively, a mechanical response dominated by plasticity can be seem, whilst the elastic recovery (associated to the area beneath the unloading portion of the IC) is very limited. Interval plots of the mechanical characterization as a function of the tanning agent are shown in Fig. 8, with error bars evaluated as measurement uncertainty at 95% confidence level, evaluated propagating contributions and ultimately dominated by measurement reproducibility[68,84]. Quantitatively, strong heteroskedasticity can be appreciated, at a confidence level of 95%, showing a significantly larger dispersion for the GLU treatment. Considering the results of topographical characterization shown in Sect. 3.7, the greater dispersion of the mechanical response GLU-tanned sample cannot be ascribed to the topography as the GLU topographical characterization is not statistically different from Cr tanning. As far as the average mechanical response, ANOVA highlights (at a confidence level of 95%) systematic differences due to the tanning treatments in the mechanical response, as it can be qualitatively appreciated in Fig. 8. Specifically, Starch and Zeolite tanning produces more elastic and softer material, whilst GLU, Al and OMW tanning induces more stiff and harder leather.

These findings align with reports on biopolymer-based tanning agents, where variations in crosslinking influenced material stiffness and durability[85]. Additionally, alternative tanning agents have been found to enhance resistance to mechanical stress, supporting their potential for industrial use[41].

Zeta potential titration curves

Figure 9 reports the zeta potential titration curves of the tested leather samples.

Figure 9 shows the pH dependence of the zeta potential of the differently tanned leather samples determined at different ionic strength of an aqueous KCl solution (dashed KCl 0.001 M, continuous lines KCl0.01 M).

Data are reported as average values of 4 measurements with relative standard deviations for each pH point. The standard deviation is an index of the material stability in the explored pH range, as previously reported by the authors[86].

The configuration of the leather plug in the measuring cell deviates significantly from the ideal condition of a flat, non-porous, and non-conductive surface for the streaming potential.

Firstly, the capillary flow path inside the leather plug is extremely irregular. Fortunately, the classical Smoluchowski equation (Eq. 1) does not require knowledge about the geometry of the flow channel but a reproducible adjustment of the sample permeability. The latter requires a control of the weight of the leather plug and its compression. The permeability is adjusted immediately after sample mounting by reducing the distance between the support disks of the cylindrical cell and by monitoring the volume flow rate of the aqueous test solution at given pressure difference between both ends of the sample plug. The dependence of the (apparent) zeta potential on the permeability of the plug-shaped sample is explained by the model of the electric double layer. The combination of the ionic strength (which determines the Debye length at the solid-water interface and thus the extension of the diffuse layer of compensating ions towards the bulk aqueous solution) and the proximity of adjacent surfaces of individual leather chips determine the applicability of the Smoluchowski equation. At low ionic strength, a small effective distance between leather surfaces leads either to an overlap of double layers and

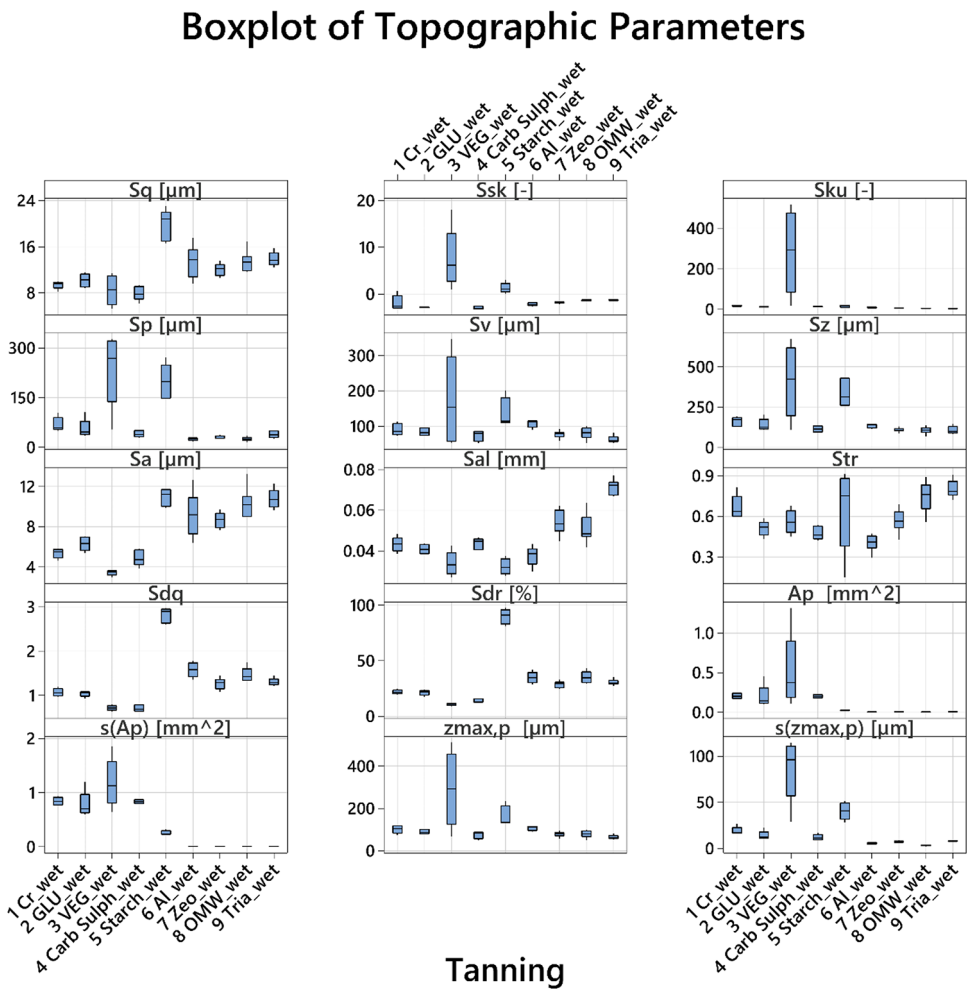


Fig. 6. Boxplots of considered topographical parameters.

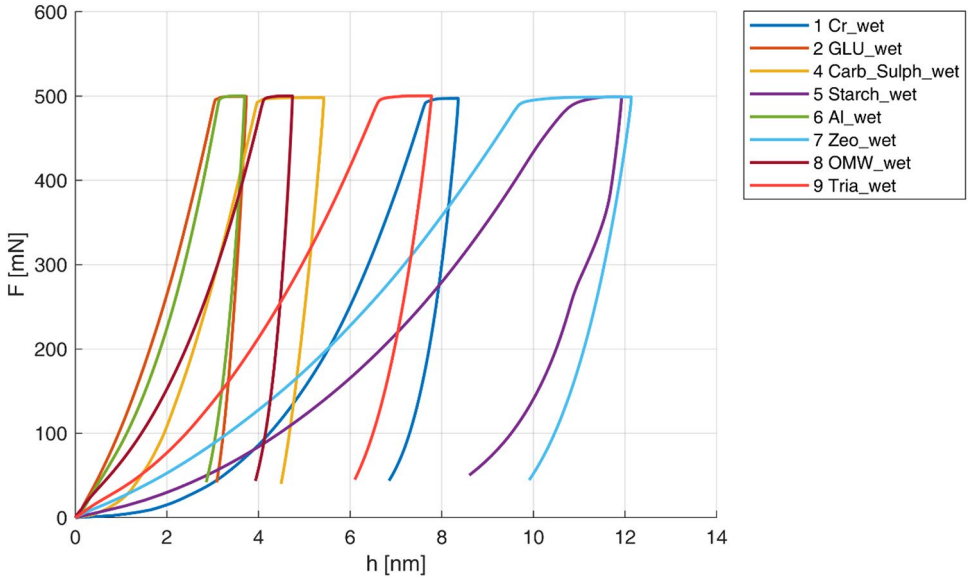


Fig. 7. Indentation curves (IC) collected by micro-IIT on starch (blue dots), Cr (red cross), GLU (green squares) and CMS (black dots). A significative difference in the mechanical response can be appreciated due to the different tanning treatments.

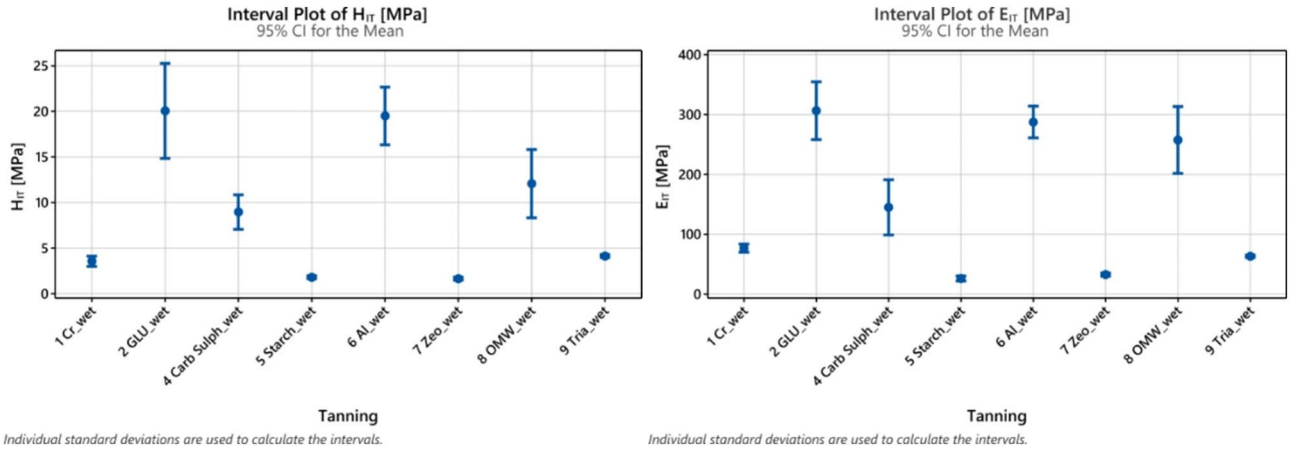


Fig. 8. (**a**) H_{IT} and (**b**) E_{IT} evaluated by micro-IIT. Systematic differences in average and dispersion can be appreciated due to the different tanning agents.

thus to a non-linear electrokinetic effect, or to a contribution of the interfacial conductance (the accumulation of ions in the diffuse layer accounts for a significantly higher conductivity compared to the bulk solution), which is not considered by the Smoluchowski equation[87]. In the latter case, the apparent zeta potential is estimated too low in magnitude[88]. Secondly, the bulk leather sample is porous and swelling in aqueous solution. Both properties introduce ionic conductance to the leather sample in its wet state. In the presence of bulk material swelling, the effect of porosity on the zeta potential is minor. Besides the introduction of ionic conductance due to water-borne ions penetrating the swollen material, swelling also let the distinct interface between the solid material surface and the surrounding aqueous solution diminish. This phenomenon shifts the shear plane at the interface towards the interior of the swollen material and further reduces the magnitude of the apparent zeta potential[89].

In order to (at least partially) compensate the adverse effects of interfacial conductance, porosity, and swelling on the determination of the zeta potential, we have selected an ionic strength of 0.01 mol/l for the aqueous KCl test solution. Although the increase in ionic strength maintains the magnitude of the Debye length (the Debye length decreases from 9.5 nm in 0.001 mol/l to 3 nm in 0.01 mol/l[72]), it does significantly reduce the adverse effect of unrecognized interfacial conductance on the zeta potential calculation. The higher ionic strength and thus the higher electrolyte conductivity further helps to better approach the ionic conductance of the wet leather sample caused by bulk material swelling. Besides, higher ionic conductance suppresses swelling compared to the low salinity condition of a 0.001 mol/l solution. Last but not least, the use of 0.01 mol/l KCl helps to maintain a reproducible electric conductivity within a wider range of pH.

Figure 9a shows the pH dependence of the zeta potential determined in 0.01 mol/l KCl for leather tanned with chromium, glutaraldehyde and dialdehyde-starch, respectively. It is easily possible to distinguish the effects of different tanning agents on the final functional groups of leather that interact with the aqueous solution and are responsible for the formation of surface charge.

The zeta potential analyses reveal an isoelectric point (IEP) at pH 5.4 for chromium-tanned leather and at pH 3.1 for glutaraldehyde-tanned leather. These values of the IEPs are consistent with the ones reported in the literature and reflect the corresponding tanning mechanisms. Chromium tanning captures available COOH groups thereby leaving an excess of free NH_2 groups that show responsible for the highest IEP in this series of tanned leather samples. Opposite, glutaraldehyde tanning involves binding of NH_2 groups such that the net surface charge and the IEP are dominated by free COOH groups[28,90]. Within the experimentally accessible pH range, it was not possible to determine the IEP of starch-tanned leather. However, the analysis of the raw measuring data, i.e., the evolution of the streaming potential coupling coefficient $dU_{str}/d\Delta p$ with electrolyte pH, suggested an IEP at pH 2.6 ± 0.1 (insert in Fig. 9). We conclude on a mechanism of tanning for the starch-based agent, which is similar to glutaraldehyde. In addition, the zeta potential of the starch-tanned leather sample may be compromised by a contribution of starch (anionic polysaccharide) that remained strongly attached to the fibrillar structure of the flesh side.

Since 0.01 M KCl gave more reliable results, new leather samples (6_Al, 7_Zeo, 8_Tria and 9_AVO) were tested only in this electrolyte. 6_Al, 7_Zeo and 9_Tria samples show an isoelectric point between 4,2 in accordance with literature values[91] Sample 8_OMW show an acidic IEP in accordance with the presence of acidic functional groups in able to link NH_2 groups of collagens leaving free COOH acidic groups. Free acidic functionalities are clearly visible from the acidic IEP and from the plateau in the basic region.

A comparison with the zeta potential results for chromium- and glutaraldehyde-tanned leather determined at the lower ionic strength of a 0.001 mol/l KCl solution reveals the complex behavior of this natural material. Firstly, the magnitude of the zeta potential is affected. A decrease in the magnitude of the zeta potential with increasing ionic strength is expected and explained by the model of the electric double layer and the compression of the diffuse layer of interfacial charge (a decrease of the Debye length). However, this decrease in magnitude is only observed for the zeta potential of glutaraldehyde-tanned leather. For chromium-tanned leather, we

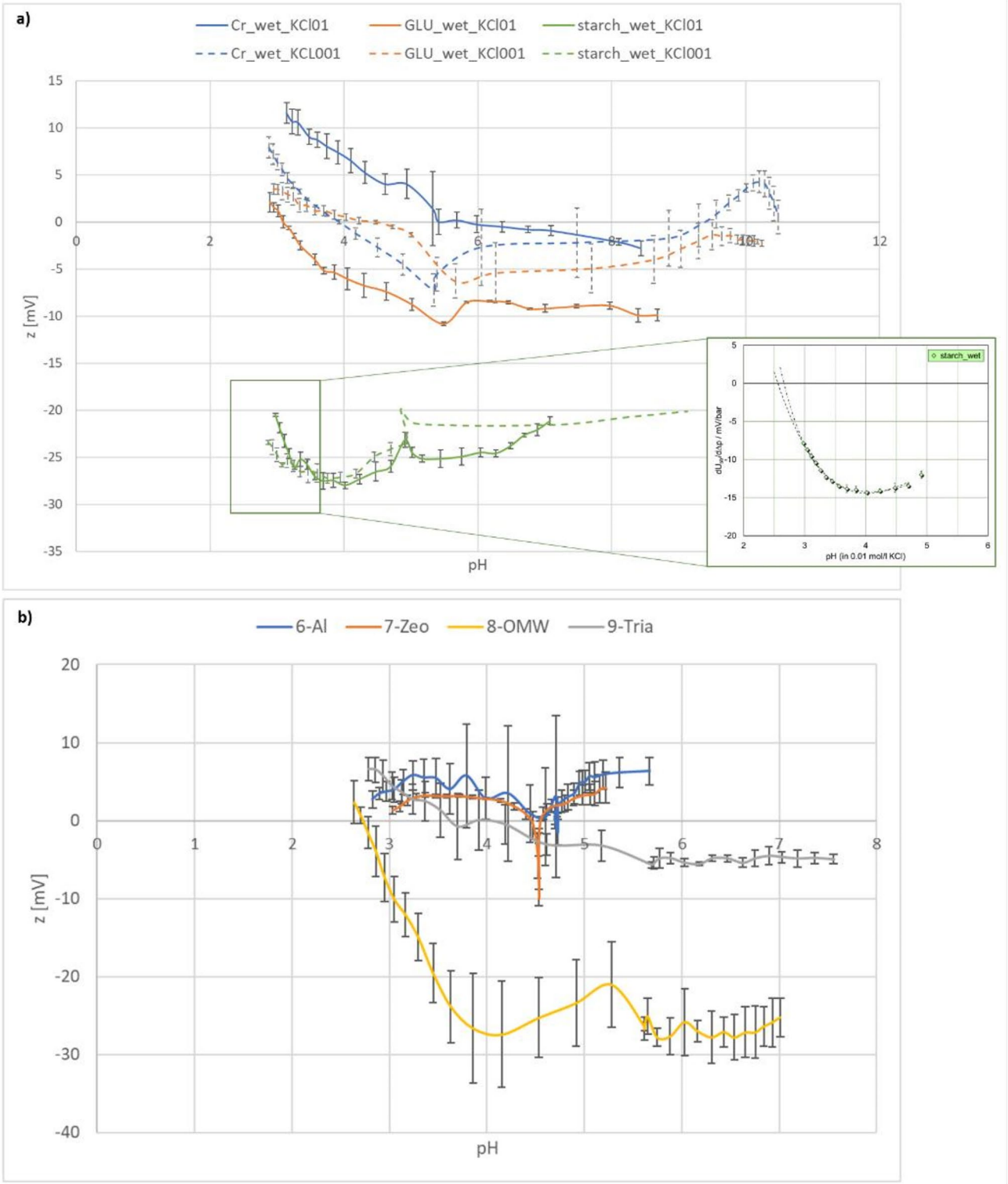


Fig. 9. (**a**) zeta potential titration curves of leather samples (Cr_wet, GLU_wet and starch_wet) determined at different ionic strength of an aqueous KCl solution (dashed KCl 0.001 M, continuous lines KCl0.01 M), (**b**) zeta potential of Al, Zeo, Tria and OMW samples in 0.01 M KCl.

observe a shift to higher negative zeta potential when changing from 0.01 mol/l to 0.001 mol/l KCl. In general, the dependence of the zeta potential on the ionic strength of a 1:1 electrolyte (such as KCl) does not affect the isoelectric point. The experimental results for tanned leather contradict this statement and suggest another process initiated by a change in the ionic strength of the aqueous test solution. As mentioned above, lower salinity enhances the swelling propensity of leather. Apparently, functional groups buried in the bulk of the

leather sample get accessible to the aqueous test solution upon swelling[92]. The distribution of COOH and NH_2 functional groups in the bulk is less affected by the tanning process and these acidic and basic groups contribute equally to the formation of surface charge. The approximation of the IEPs for chromium- and glutaraldehyde-tanned leather samples in 0.001 mol/l KCl confirm this hypothesis. Secondly, the higher degree of swelling of leather in low ionic strength condition is reflected by the reverse trend of the zeta potential at higher pH. While in 0.01 mol/l KCl, chromium-tanned leather shows a steady increase in the negative zeta potential and glutaraldehyde-tanned leather exhibits a plateau zeta potential above pH 5, the magnitude of the (apparent) zeta potential decreases in the alkaline range when leather gets exposed to the lower ionic strength of 0.001 mol/l. This indication of swelling by the pH dependence of the apparent zeta potential is also observed for natural fibers[93]. In conclusion, the selection of the higher ionic strength of 0.01 mol/l eliminates the effects of a series of physical artefacts on the determination of the zeta potential and makes differently tanned leather samples better distinguishable.

Conclusion

Leather samples at the wet state, coming from traditional (e.g. Chrome and Glutaraldehyde) and innovative (e.g. vegetable, carbamoyl sulphate, starch and OMW) tanning processes have been deeply characterized from the physical and chemical standpoints. Well established characterizations, such as optical microscopy, shrinkage temperature, wettability, metal content, infrared spectroscopy and X-ray diffraction, have been applied. In addition, new and unconventional methods for the leather field, such as surface topography characterization, instrumented indentation and zeta potential electrokinetic measurements were applied and optimized for this type of samples.

The first goal achieved by this research is the design and optimization of a set of characterization techniques suitable for the analysis and comparison of leather samples at the wet state from different tanning processes.

The explored techniques were able to highlight differences among the different tanning process which can be correlated with the different mechanisms of tanning and which can increase the knowledge about the process and the effectiveness of innovative methods.

In particular Optical microscopy allows the visualization of grain and dermis structure to investigate and compare products properties and eventual defects. Advanced topographical measurements supported optical microscopy with a new and also quantitative method for the investigation of surface morphology and eventual defects. Moreover, instrumented indentation can add significant information related to surface mechanical properties and elasticity correlated with product quality and performances.

Shrinkage temperature measures the ability of a tanning process to stabilize collagen. This measurement is properly supported by XRD evaluation which investigates collagen structure.

A deep insight in molecular interactions and possible changes in collagen structure is given by FTIR-ATR analysis and for the first time by zeta potential measurements. The combination of these two techniques allows the investigation of functional groups exposed by tanned samples giving information about the ones involved in the tanning process and consequently on the tanning mechanism.

Finally, the evaluation of metal content is fundamental for leather classification but also for the evaluation of possible health and environmental concerns in certain processing technologies.

The knowledge of mechanisms and features of different tanning processes are crucial for the optimization of the subsequent steps of leather processing specific for each tanning agent reducing defects. Moreover, a quantitative and objective comparison among different tanning processes allows the design and development of technologies with reduced health and environmental impact.

Data availability

Data availability: The raw/processed data required to reproduce these findings are available upon request to Sara Ferraris (sara.ferraris@polito.it).

Received: 23 December 2024; Accepted: 14 March 2025
Published online: 27 March 2025

References

1. UNIC Sustainability Report 2022.
2. UNIC Business overview. on Italian tanning industry (2022).
3. Li, L. & Zhang, M. The efficient extraction method of collagen from deteriorated leather artifacts. *Polymers* **15**, 3459. https://doi.org/10.3390/polym15163459 (2023).
4. Masilamani, D., Ariram, N., Madhan, B. & Palanivel, S. An integrated process for effective utilization of collagenous protein from Raw Hide trimmings: valorization of tannery solid wastes. *J. Clean. Prod.* **415**, 137705. https://doi.org/10.1016/j.jclepro.2023.137705 (2023).
5. Maistrenko, L. et al. Collagen obtained from leather production waste provides suitable gels for biomedical applications. *Polymers* **14**, 4749. https://doi.org/10.3390/polym14214749 (2022).
6. Wan, J. et al. Bioinspired Paper-Based nanocomposites enabled by Biowax–Mineral hybrids and proteins. *ACS Sustainable Chem. Eng.* **8**, 26, 9906–9919. https://doi.org/10.1021/acssuschemeng.0c03187 (2020).
7. Solihat, N. N. et al. Recent antibacterial agents from biomass derivatives: characteristics and applications. *J. Bioresour Bioprod.* **9**, 283–309. https://doi.org/10.1016/j.jobab.2024.02.002 (2024).
8. Alemu, L. G. et al. Toward sustainable leather processing: A comprehensive review of cleaner production strategies and environmental impacts. *Adv. Mater. Sci. Eng.*, 117915. https://doi.org/10.1155/2024/8117915 (2024).
9. Hao, D. et al. Sustainable leather making — An amphoteric organic chrome-free tanning agents based on recycling waste leather. *Sci. Total Environ.* **867**, 161531. https://doi.org/10.1016/j.scitotenv.2023.161531 (2023).
10. Lasoń-Rydel, M., Sieczyńska, K., Gendaszewska, D., Ławińska, K. & Olejnik, T. Use of enzymatic processes in the tanning of leather materials. *AUTEX Res. J.* **24** (Issue 1), 20230012. https://doi.org/10.1515/aut-2023-0012 (2024).

11. Teklemedhin, T. B. et al. Vegetable tannins as chrome-free leather tanning. *Adv. Mater. Sci. Eng.*, 220778. https://doi.org/10.1155/2023/6220778 (2023).
12. Kanth, S. V. et al. Studies on the use of enzymes in tanning process: part II. Kinetics of vegetable tanning process. *J. Am. Leather Chem. Assoc.* **105**, 16–24 (2010).
13. Falcão, L. & Araújo, M. E. M. Vegetable tannins used in the manufacture of historic leathers. *Molecules* **23**, 1081. https://doi.org/10.3390/molecules23051081 (2018).
14. Anggriyani, E., Rachmawati, L. & Adetya, N. P. The use of non-chrome mineral tanning materials as a preferable environmentally friendly tanning material. *Revista De Pielărie Încălțăminte*. **21**, 3 (2021).
15. Florio, C., Naviglio, B. & Calvanese, G. Advanced approaches in leather research using X-ray probe equipped SEM microscopy. *SLTC J.* **101**, 165–172 (2011).
16. Florio, C., Aveta, R., Calvanese, G. & Naviglio, B. Advanced diagnostic and innovative solutions for Letaher defects: the problem of yellowing. *SLTC J.* **103**, 296–304 (2019).
17. Florio, C. & Calvanese, G. Light dependent properties of finishing and leather defects. *Adv. Mater. Phys. Chem.* **11**, 243–253 (2021).
18. Serrano-Lotina, A. et al. Zeta potential as a tool for functional materials development. *Catal. Today*. **423**, 113862. https://doi.org/10.1016/j.cattod.2022.08.004 (2023).
19. Kamble, S. et al. Revisiting zeta potential, the key feature of interfacial phenomena, with applications and recent advancements. *Chem. Select* **7**, e202103084 (2022).
20. Metwally, S. & Stachewicz, U. Surface potential and charges impact on cell responses on biomaterials interfaces for medical applications. *Mat. Sci. Eng. C.* **104**, 109883 (2019).
21. Spriano, S. et al. How do wettability, zeta potential and hydroxylation degree affect the biological response of biomaterials? *Mat. Sci. Eng. C.* **74**, 542–555 (2017).
22. Dukhin, A. S. & Xu, R. Zeta-potential measurements. In Micro and Nano Technologies, Characterization of Nanoparticles (V.-D. Hodoroaba, W. E. S. Unger, A. G. Shard eds), 213–224 (Elsevier, 2020). https://doi.org/10.1016/B978-0-12-814182-3.00014-6
23. Luxbacher, T. *The ZETA Guide: Principles of the Streaming Potential Technique* (Anton Paar, 2014).
24. Covington, A. D. Prediction in leather processing: a dark Art or a clear possibility? *JSLTC* **95**, 231–242 (2011).
25. Song, Y., Wang, Y., Zeng, Y., Wu, H. & Shi, B. Quantitative determinations of isoelectric point of retanned leather and distribution of retanning agent. *JALCA* **113**, 232–238 (2018).
26. Wang, Y. & Hu, L. Essential role of isoelectric point of skin/leather in leather processing. *J. Leather Sci. Eng.* **4**, 25. https://doi.org/10.1186/s42825-022-00099-y (2022).
27. Wise, W. R. et al. Zeolites as sustainable alternatives to traditional tanning chemistries. *Green. Chem.* **25**, 4260–4270. https://doi.org/10.1039/d3gc00381g (2023).
28. Wang, Y. et al. *Surface Charge and Isoelectric Point of Leather: A Novel Determination Method and its Application in Leather Making*, vol. 112, 223–224 (JALCA, 2017).
29. Jawahar, M., Babu, N. K. C., Vani, K., Jani Anbarasi, L. & Geetha, S. Vision based inspection system for leather surface defect detection using fast convergence particle swarm optimization ensemble classifier approach. *Multimed Tools Appl.* **80**, 4203–4235. https://doi.org/10.1007/s11042-020-09727-3 (2021).
30. Mullany, B., Savio, E., Haitjema, H. & Leach, R. The implication and evaluation of geometrical imperfections on manufactured surfaces. *CIRP Ann.* **71**, 717–739. https://doi.org/10.1016/j.cirp.2022.05.004 (2022).
31. Chiba, T., Kuroda, S. & Yamaguchi, M. Modeling the relationship between tactile sensation and physical properties of synthetic leather. *J. Ind. Text.* **50**, 346–363. https://doi.org/10.1177/1528083719830141 (2020).
32. Leach, R. K. *Optical Measurement of Surface Topography* (Springer, 2011). https://doi.org/10.1007/978-3-642-12012-1
33. ISO 25178-2:2021 Geometrical Product Specifications (GPS) Surface Texture: Areal Part 2: Terms, definitions and surface texture parameters.
34. Štěpánová, V. et al. Surface modification of natural leather using diffuse ambient air plasma. *Int. J. Adhes. Adhes.* **77**, 198–203. https://doi.org/10.1016/j.ijadhadh.2017.05.004 (2017).
35. Mihai, A., Seul, A., Curteza, A. & Costea, M. Mechanical parameters of leather in relation to technological processing of the footwear uppers. *Materials* **15**, 5107. https://doi.org/10.3390/ma15155107 (2022).
36. ISO 3376:2020 | IULTCS/IUP 6 Leather Physical and Mechanical Tests Determination of tensile strength and percentage elongation.
37. ISO 14577-1:2015 Metallic materials Instrumented indentation test for hardness and materials parameters, Part 1: Test method.
38. Lucca, D. A., Herrmann, K. & Klopfstein, M. J. Nanoindentation: measuring methods and applications. *CIRP Ann.* **59**, 803–819. https://doi.org/10.1016/j.cirp.2010.05.009 (2010).
39. Oliver, W. C. & Pharr, G. M. Measurement of hardness and elastic modulus by instrumented indentation: advances in Understanding and refinements to methodology. *J. Mater. Res.* **19**, 3–20 (2004).
40. Dang, X. et al. β-Cyclodextrin-Based Chrome-Free tanning agent results in the sustainable and cleaner production of Eco-Leather. *ACS Sustainable Chem. Eng.* **12**, 3715–3725. https://doi.org/10.1021/acssuschemeng.3c07446 (2024).
41. Hao, D. et al. A wrench-like green amphoteric organic chrome-free tanning agent provides long-term and effective antibacterial protection for leather. *J. Clean. Prod.* **404**, 136917. https://doi.org/10.1016/j.jclepro.2023.136917 (2023a).
42. Wang, X., Su, R., Hao, D. & Dang, X. Sustainable utilization of corn starch resources: A novel soluble starch-based functional chrome-free tanning agent for the eco-leather production. *Ind. Crops Prod.* **187**, 115534. https://doi.org/10.1016/j.indcrop.2022.115534 (2022).
43. Hao, D. et al. Chrome-free tanning agent based on epoxy-modified dialdehyde starch towards sustainable leather making. *Green. Chem.* **23**, 9693–9703. https://doi.org/10.1039/D1GC03472C (2021).
44. Hao, D. et al. Sustainable leather making — An amphoteric organic chrome-free tanning agents based on recycling waste leather. *Sci. Total Environ.* **867**, 161531. https://doi.org/10.1016/j.scitotenv.2023.161531 (2023b).
45. Shen, J. & Zhang, M. Disassembly, refinement, and reassembly: from ancient papermaking to modern materials processing. *J. Bioresources Bioprod.* **10**, 7–13. https://doi.org/10.1016/j.jobab.2024.11.002 (2025).
46. Ozkan, C. K. & Ozgunay, H. *Usage of Starch in Leather Making, Conference: The 6th International Conference on Advanced Materials and Systems*. https://doi.org/10.24264/icams-2016.IV.10 (2016).
47. ISO 3380:2015 Determination of shrinkage temperature up to 100°C (IULTCS/IUP 16).
48. ISO 17072-2:2022Chemical Determination of Metal content - Part 2: Total metal content.
49. ASTM standard. Test Method for Surface Wettability D, 724–799.
50. Florio, C., Mascolo, R., Calvanese, G. & Naviglio, B. The role of surface properties in durability and comfort of finished leathers - XXXIII IULTCS CONGRESS, Novo Hamburgo, (BRASILE) **92**(6), 323–330. (2015).
51. Florio, C. et al. Improving electrical conductivity of leather surface: a new technology versus industrial applications. *Nano Express*, **1**, 010032. (2020).
52. Fierro, F. et al. Multifunctional leather finishing vs. applications, through the addition of well–dispersed flower–like nanoparticles -. *Sci. Rep.* **14**, 2163. https://doi.org/10.1038/s41598-024-51775-4 (2024).
53. de Groot, P. Coherence scanning interferometry. In Optical Measurement of Surface Topography (ed Leach, R.). https://doi.org/10.1007/978-3-642-12012-1_9 (Springer, 2011).
54. ISO 25178-604:2013 Geometrical product specifications (GPS) Surface texture: Areal. Part 604: Nominal characteristics of non-contact (coherence scanning interferometry) instruments.

55. Giusca, C. L., Leach, R. K., Helary, F., Gutauskas, T. & Nimishakavi, L. Calibration of the scales of areal surface topography measuring instruments: part 1. Measurement noise and residual flatness. *Meas. Sci. Technol.* **23**, 035008. https://doi.org/10.1088/0957-0233/23/3/035008 (2012).
56. Giusca, C. L., Leach, R. K. & Helery, F. Calibration of the scales of areal surface topography measuring instruments: part 2. Amplification, linearity and squareness. *Meas. Sci. Technol.* **23**, 065005. https://doi.org/10.1088/0957-0233/23/6/065005 (2012b).
57. ISO 25178-3:2012 Geometrical Product Specifications (GPS) Surface Texture: Areal Part 3: Specification operators.
58. Leach, R. & Haitjema, H. Bandwidth characteristics and comparisons of surface texture measuring instruments. *Meas. Sci. Technol.* **21**, 032001. https://doi.org/10.1088/0957-233/21/3/032001 (2010).
59. Maculotti, G., Feng, X., Su, R., Galetto, M. & Leach, R. Residual flatness and scale calibration for a point autofocus surface topography measuring instrument. *Meas. Sci. Technol.* **30**, 075005. https://doi.org/10.1088/1361-6501/ab188f (2019).
60. Maculotti, G., Pistone, G. & Vicario, G. Inference on errors in industrial parts: kriging and variogram versus geometrical product specifications standard. *Appl. Stoch. Models Bus. Ind.* **37**, 839–858. https://doi.org/10.1002/asmb.2603 (2021).
61. Ghibaudo, C. et al. Information-rich quality controls prediction model based on non-destructive analysis for porosity determination of AISI H13 produced by electron beam melting. *Int. J. Adv. Manuf. Technol.* **126**, 1159–1173. https://doi.org/10.1007/s00170-023-11153-2 (2023).
62. Maculotti, G., Ghibaudo, C., Genta, G., Ugues, D. & Galetto, M. An artificial intelligence classifier for electron beam powder bed fusion as-built surface topographies. *CIRP J. Manuf. Sc Technol.* **43**, 129–142. https://doi.org/10.1016/j.cirpj.2023.03.006 (2023).
63. Quagliotti, D. Modeling the systematic behavior at the micro and nano length scales. *Surf. Topogr : Metrol. Prop.* **10**, 015011. https://doi.org/10.1088/2051-672X/ac4ba7 (2022).
64. Corder, G. W. & Foreman, D. I. *Nonparametric Statistics: A Step-by-Step Approach*. (Wiley, 2014). ISBN 978-1118840313.
65. Galetto, M., Kholkhujaev, J. & Maculotti, G. Improvement of instrumented indentation test accuracy by data augmentation with electrical contact resistance. *CIRP Ann.* **72**, 469–472. https://doi.org/10.1016/j.cirp.2023.03.034 (2023).
66. Kholkhujaev, J., Maculotti, G., Genta, G. & Galetto, M. Metrological comparison of available methods to correct Edge-Effect local plasticity in instrumented indentation test. *Materials* **16**, 4262. https://doi.org/10.3390/ma16124262 (2023).
67. Galetto, M., Genta, G. & Maculotti, G. Single-step calibration method for nano indentation testing machines. *CIRP Ann.* **69**, 429–432. https://doi.org/10.1016/j.cirp.2020.03.015 (2020).
68. Maculotti, G., Genta, G. & Galetto, M. An uncertainty-based quality evaluation tool for nanoindentation systems. *Measurement* **225**, 113974. https://doi.org/10.1016/j.measurement.2023.113974 (2024).
69. ISO 14577-2:2015 Metallic Materials Instrumented Indentation Test for Hardness and Materials Parameters Part 2: Verification and calibration of testing machines.
70. Chudoba, T. & Richter, F. Investigation of creep behaviour under load during indentation experiments and its influence on hardness and modulus results. *Surf. Coat. Technol.* **148**, 191–198. https://doi.org/10.1016/S0257-8972(01)01340-8 (2001).
71. Montgomery, D. C. *Design and Analysis of Experiments*, 10th Edition (Wiley, 2019). ISBN: 978-1-119-49244-3.
72. Hunter, R. J. *Zeta Potential in Colloid Science* (Academic, 1981).
73. Ferraris, S., Gamna, F., Nogarole, M. & Florio, C. Zeta potential electrokinetic measurements on solid samples: potentialities in the leather field. *CPMC* **3**, 38–43 (2023).
74. UNI EN ISO. 15987:2015Cuoio - Terminologia - Definizioni chiave per il commercio del cuoio.
75. UNI EN ISO 17075-. 2 Chemical Determination of chromium(VI) Content in leather - Part 2: Chromatographic method.
76. Radev, L., Hristov, V., Samuneva, B. & Ivanova, D. Organic/Inorganic bioactive materials part II: in vitro bioactivity of Collagen-Calcium phosphate silicate/wollastonite hybrids, cent. *Eur. J. Chem.* **7**, 711–720. https://doi.org/10.2478/s11532-009-0076-1 (2009).
77. Stani, C., Vaccari, L., Mitri, E. & Birarda, G. FTIR investigation of the secondary structure of type I collagen: new insight into the amide III band. *Spectrochim Acta Part. A.* **229**, 118006. https://doi.org/10.1016/j.saa.2019.118006 (2020).
78. Hedberg, Y. S., Lidén, C. & Odnevall Wallinder, I. Correlation between bulk- and surface chemistry of Cr-tanned leather and the release of Cr(III) and Cr(VI). *J. Hazard. Mater.* **21**, 285:542. https://doi.org/10.1016/j.jhazmat.2014.08.061 (2015).
79. Carsote, C., Sendrea, C., Micu, M-C., Adams, A. & Badea, E. Micro-DSC, FTIR-ATR and NMR MOUSE study of the dose-dependent effects of gamma irradiation on vegetable-tanned leather: the influence of leather thermal stability. *Radiat. Phys. Chem.* **189**, 109712 (2021).
80. Badea, E., Carşote, C., Hadîmbu, E., Şendrea, C. & Lupaş, M. C. The effect of Halloysite nanotubes dispersions on vegetable-tanned leather thermal stability. *Herit. Sci.* **7**, 68. https://doi.org/10.1186/s40494-019-0310-x (2019).
81. Zhang, J. & Chen, W. A faster and more effective Chrome tanning process assisted by microwave. *RSC Adv.* **10**, 23503 (2020).
82. Brudzynska, P., Sionkowska, A. & Grisel, M. Leather dyeing by Plant-Derived colorants in the presence of natural additives. *Materials* **15**, 3326. https://doi.org/10.3390/ma15093326 (2022).
83. Thongchai, K., Chuysinuan, P., Thanyacharoen, T., Techasakul, S. & Ummartyotin, S. Integration of collagen into Chitosan blend film composites: physicochemical property aspects for pharmaceutical materials. *SN Appl. Sci.* **2**, 255. https://doi.org/10.1007/s42452-020-2052-5 (2020).
84. Barbato, G. et al. Uncertainty evaluation of indentation modulus in the nano-range: contact stiffness contribution. *CIRO Ann.* **66**, 495–498. https://doi.org/10.1016/j.cirp.2017.04.060 (2017).
85. Dang, X. et al. β-Cyclodextrin-Based Chrome-Free tanning agent results in the sustainable and cleaner production of Eco-Leather. *ACS Sustainable Chem. Eng.* **12**, 9, 3715–3725 (2024).
86. Ferraris, S. et al. The mechanical and chemical stability of the interfaces in bioactive materials: the substrate-bioactive surface layer and hydroxyapatite bioactive surface layer interfaces. *Mater. Sci. Eng. C.* **116**, 111238 (2020).
87. Lyklema, J. & Minor, M. On surface conduction and its role in electrokinetics. *Colloids Surf. A.* **140**, 33–41. https://doi.org/10.1016/S0927-7757(97)00266-5 (1998).
88. Werner, C., Körber, H., Zimmermann, R., Dukhin, S. & Jacobasch, H-J. Extended electrokinetic characterization of flat solid surfaces. *J. Colloid Interface Sci.* **208**, 329–346. https://doi.org/10.1006/jcis.1998.5787 (1998).
89. Stana-Kleinschek, K., Kreze, T., Ribitsch, V. & Strnad, S. Reactivity and electrokinetical properties of different types of regenerated cellulose fibres. *Colloids Surf. A.* **195**, 275–284. https://doi.org/10.1016/S0927-7757(01)00852-4 (2001).
90. Guthrie-Strachan, J. & Flowers, K. Protein and leather charge. *World Leather.* **18**, 19–23 (2005).
91. Wise, W. R. et al. Zeolites as sustainable alternatives to traditional tanning chemistries. *Green. Chem.* **25**, 4260 (2023).
92. Freudenberg, U. et al. Electrostatic interactions modulate the conformation of collagen I. *Biophys. J.*, **92**, 2108–2119, https://doi.org/10.1529/biophysj.106.094284 (2007).
93. Bismarck, A. et al. Surface characterization of flax, hemp and cellulose fibers; surface properties and the water uptake behavior. *Polym. Compos.* **23**, 872–894. https://doi.org/10.1002/pc.10485 (2002).

Acknowledgements

This study was carried out within the MICS (Made in Italy–Circular and Sustainable) Extended Partnership and received funding from the European Union Next-Generation EU (PIANO NAZIONALE DI RIPRESA E RESILIENZA (PNRR) –MISSIONE 4 COMPONENTE 2, INVESTIMENTO 1.3 –D.D. 1551.11-10-2022, PE00000004). This manuscript reflects only the authors' views and opinions, neither the European Union nor

the European Commission can be considered responsible for them.

Author contributions

Conceptualization: SF, MN, CFData Curation: SF, FG, TL, GM, JK, GG, AS, LGFormal Analysis: SF, FG, GM, CFFunding Acquisition: SF, MG, CFInvestigation: SF, FG, TL, GM, JK, MN, AS, LGMethodology: SF, FG, TL, GM, GG, MN, CFProject Administration: SF, MG, CFResouces: SF, MG, MN, CFSupervision: SF, GG, MG, CFValidation: SF, FG, TL, GM, CFVisualization: SF, FG, GM, JK, AS, LGWriting original draft: SF, FG, TL, GM, JK, GG, CFWiting revision and editing: SF, FG, TL, GM, JK, GG, MG, MN, CF, AS, LG.

Declarations

Competing interests

The authors declare no competing interests.

Additional information

Correspondence and requests for materials should be addressed to S.F.

Reprints and permissions information is available at www.nature.com/reprints.

Publisher's note Springer Nature remains neutral with regard to jurisdictional claims in published maps and institutional affiliations.

Open Access This article is licensed under a Creative Commons Attribution-NonCommercial-NoDerivatives 4.0 International License, which permits any non-commercial use, sharing, distribution and reproduction in any medium or format, as long as you give appropriate credit to the original author(s) and the source, provide a link to the Creative Commons licence, and indicate if you modified the licensed material. You do not have permission under this licence to share adapted material derived from this article or parts of it. The images or other third party material in this article are included in the article's Creative Commons licence, unless indicated otherwise in a credit line to the material. If material is not included in the article's Creative Commons licence and your intended use is not permitted by statutory regulation or exceeds the permitted use, you will need to obtain permission directly from the copyright holder. To view a copy of this licence, visit http://creativecommons.org/licenses/by-nc-nd/4.0/.

© The Author(s) 2025